C. R. Physique 17 (2016) 543–554

Contents lists available at ScienceDirect

Comptes Rendus Physique

www.sciencedirect.com

Phononic crystals / Cristaux phononiques

# Nonlinear propagation and control of acoustic waves in phononic superlattices

## *Propagation non linéaire et contrôle des ondes acoustiques dans les super-réseaux phononiques*

Noé Jiménez [a,*], Ahmed Mehrem [a], Rubén Picó [a], Lluís M. García-Raffi [b], Víctor J. Sánchez-Morcillo [a]

[a] *Instituto de Investigación para la Gestión Integrada de Zonas Costeras, Universitat Politècnica de València, Paranimf 1, 46730 Grao de Gandia, Spain*
[b] *Instituto de Matemática Pura y Aplicada, Universitat Politècnica de València, Cami de Vera s/n, 46022, Valencia, Spain*

ARTICLE INFO

*Article history:*
Available online 28 February 2016

*Keywords:*
Nonlinear
Phononic
Multilayer

*Mots-clés :*
Non-linéarité
Phononique
Multicouche

ABSTRACT

The propagation of intense acoustic waves in a one-dimensional phononic crystal is studied. The medium consists in a structured fluid, formed by a periodic array of fluid layers with alternating linear acoustic properties and quadratic nonlinearity coefficient. The spacing between layers is of the order of the wavelength, therefore Bragg effects such as band gaps appear. We show that the interplay between strong dispersion and nonlinearity leads to new scenarios of wave propagation. The classical waveform distortion process typical of intense acoustic waves in homogeneous media can be strongly altered when nonlinearly generated harmonics lie inside or close to band gaps. This allows the possibility of engineer a medium in order to get a particular waveform. Examples of this include the design of media with effective (e.g., cubic) nonlinearities, or extremely linear media (where distortion can be canceled). The presented ideas open a way towards the control of acoustic wave propagation in nonlinear regime.



RÉSUMÉ

La propagation d'ondes acoustiques intenses dans un cristal phononique à une dimension est étudiée. Le milieu consiste en un fluide structuré, formé par un réseau périodique de couches fluides dont les propriétés acoustiques linéaires ainsi que le coefficient de non-linéarité quadratique sont alternés. L'espacement entre les couches est de l'ordre de la longueur d'onde ; en conséquence, des effets de type Bragg tels que des bandes interdites apparaissent. Nous montrons que l'interaction entre la dispersion forte et la non-linéarité conduit à de nouveaux scénarios de propagation d'ondes. Le processus classique de distorsion de la forme d'onde, typique des ondes acoustiques intenses dans les milieux homogènes, peut être fortement altéré quand des harmoniques générées de manière non linéaire se retrouvent à l'intérieur des bandes interdites ou au voisinage de celles-ci.

* Corresponding author.
*E-mail address:* nojigon@upv.es (N. Jiménez).

http://dx.doi.org/10.1016/j.crhy.2016.02.004

Ceci offre la possibilité de façonner un milieu de manière à obtenir une forme d'onde particulière. Les exemples donnés incluent la réalisation de milieux avec des non-linéarités effectives (par exemple, cubiques), ou de milieux extrêmement linéaires (où la distorsion peut être annulée). Les idées présentées ouvrent la voie au contrôle de la propagation des ondes acoustiques en régime non linéaire.



## 1. Introduction

One of the most celebrated effects of wave propagation in periodic media is the appearance of forbidden propagation regions in the energy spectrum of electrons, or band gaps. Most of the physics of semiconductors, and therefore many electronic devices, are somehow based on this concept [1]. In the late 1980's, these ideas where extended by Yablonovich and John [2] to light waves (electromagnetic waves in general) propagating in materials where the optical properties like the index of refraction were distributed periodically. These materials were named, by analogy with ordered atoms in crystalline matter, as photonic crystals. The typical scale of the periodicity is given by the wavelength. Actually, not only light but any wave propagating in a periodic medium may experience the same effects, and acoustic waves are not an exception. Sound wave propagation in periodic media has become very popular in the last 20 years in acoustics, after the introduction of the concept of sonic crystals [3]. Exploiting the analogies with other types of waves many interesting effects, as the above-mentioned forbidden propagation bands (band gaps), but also focalization, self-collimation, negative refraction, and many others have been proposed. We consider in this paper the simplest case of plane waves propagating in a 1D structure, formed by a periodic alternation of layers with different properties. Depending on the context, such a structure has been named a multilayer, a superlattice (particularly in the context of semiconductors) or a 1D phononic crystal (this include more exotic structures, as the granular crystal or lattice [4]).

The huge majority of the studies considered so far have assumed a low-amplitude (linear) regime, neglecting the nonlinear response of the medium. Intense wave propagation in nonlinear periodic media, and in particular the case of sound waves, is almost unexplored. In this paper, we present new phenomena related to acoustic wave propagation in a 1D periodic media, where both layers have a nonlinear quadratic elastic response. Nonlinear acoustic effects in such a structure have been studied only in a few works. In [5], the harmonic generation process is described in a fluid/fluid multilayered structure (water/glycerin), based in a nonlinear wave equation. Also, acoustic solitons in solid layered nonlinear media have been presented in [6]. The complementary action of nonlinearity and periodicity has been considered in [7], where an asymmetric propagation device (acoustic diode) was proposed. There, the nonlinearity and the periodicity effects on propagation are produced at different locations and its effect is considered separately. Recently, the authors studied the conditions for the efficient generation of a narrow, nondiverging beam of second harmonic in [8].

The physical phenomena discussed in this paper are the result of the interplay between nonlinearity and periodicity. Harmonic generation effects in nonlinear monoatomic (granular) lattices were recently reported by some of us in [4]. Here we describe how the geometrical and acoustic parameters of the structure can be used to control the harmonic distortion processes in a multilayer. The particular conditions required to selectively act on the nonlinearly generated spectrum, and therefore manipulate the waveform in the specific way, are presented and discussed.

The theory presented here has been developed for fluid–fluid (scalar) structures; however, the main conclusions are extendable to fluid–solid or to solid–solid multilayers, if particular conditions are given. Also, the main conclusions of this paper are independent of the frequency regime and the propagation medium of the waves (audible, ultrasound...), and therefore of the size or scale of the structure. Specially interesting is the domain when ultrasound waves belong to the Terahertz regime, where these ideas may find a great potential. The progress in miniaturization and the technological development allows us currently to create phononic multilayers at scales even in the nanometer range (each layer contains then a small number of atoms). This structures are usually made of semiconductors and are often used in particular applications as phononic mirrors to form phonon nanocavities [9], or microcavities to obtain a strong optomechanical coupling [10] (for a survey, see [11]). In a remarkable recent achievement, acoustic amplification was realized in doped GaAs/AlAs superlattices, where a SASER (Sound Amplification by the Stimulated Acoustic phonon Radiation) was demonstrated, in a device including a superlattice gain medium and GaAs/AlAs SLs acoustic mirrors [12].

The structure of the paper is as follows: in Sec. 2, we present the model for nonlinear propagation of acoustic waves in periodic media. The next Sec. 3 describes the process of harmonic generation in homogeneous media, and how it is modified by the presence of periodicity. In Sec. 4, the manipulation of the spectrum of a propagating sound wave by tuning the parameters of the layered medium is discussed. Examples of a particular case, as the case of a cubic-effective medium made out of quadratically nonlinear layers are shown. Finally, Sec. 5 presents the conclusions.

## 2. The model

### 2.1. Nonlinear constitutive model

The nonlinear propagation of acoustic waves in inhomogeneous media can be described by several models with different levels of accuracy. Here, we use the equations of continuum mechanics for ideal fluids with space-dependent parameters. These are the continuity equation for mass conservation [13]:

$$\frac{\partial \rho}{\partial t} + \nabla \cdot (\rho \mathbf{v}) = 0 \tag{1}$$

and the equation of motion that follows from the conservation of momentum

$$\rho \frac{\mathrm{D}\mathbf{v}}{\mathrm{D}t} + \nabla p = 0 \tag{2}$$

where $\rho$ is the total density, $\mathbf{v}$ is the particle velocity vector over a Eulerian reference frame, $p$ is the acoustic pressure, $t$ is time and D is the material derivative operator, defined by $\frac{\partial \mathrm{D}}{\partial t} \equiv \frac{\partial}{\partial t} + (\mathbf{v} \cdot \nabla)$.

For non-homogeneous media, the ambient properties of the fluid in the absence of sound are space dependent, so the total density becomes $\rho(t, \mathbf{x}) = \rho'(t, \mathbf{x}) + \rho_0(\mathbf{x})$, where $\rho_0(\mathbf{x})$ is the spatially dependent ambient density and $\rho'(t, \mathbf{x})$ is the perturbation of the density or acoustic density, that is space and time dependent. Then, using the material derivative, Eq. (2) becomes

$$\rho_0 \frac{\partial \mathbf{v}}{\partial t} + \nabla p = -\rho' \frac{\partial \mathbf{v}}{\partial t} - \left(\rho' + \rho_0\right)(\mathbf{v} \cdot \nabla)\,\mathbf{v} \tag{3}$$

In this equation, the first two terms in the left-hand side account for linear acoustic propagation, and the terms in the right-hand side introduce nonlinearity in the Eulerian reference frame through momentum advection processes.

Eq. (1) can be expanded for non-homogeneous media as:

$$\frac{\partial \rho'}{\partial t} + \rho_0 \nabla \cdot \mathbf{v} + \mathbf{v} \cdot \nabla \rho_0 = -\rho' \nabla \cdot \mathbf{v} - \mathbf{v} \cdot \nabla \rho' \tag{4}$$

Here, the first two terms in the left-hand side account for linear acoustic propagation, the third, also linear, accounts for the magnitude of the changes in the ambient layer properties. Note that this term is space dependent, but only changes at the interface between adjacent layers. For density matched layers, $\rho_i = \rho_{i-1}$, this terms vanishes. The terms on the right-hand side are nonlinear and accounts for mass advection.

Finally, a fluid thermodynamic state equation $p = p(\rho)$ is needed to close the system. The local nonlinear medium response relating density and pressure variations, retaining up to second order terms, can be written as

$$p = c_0^2 \rho' + \frac{B}{2A} \frac{c_0^2}{\rho_0} \rho'^2 \tag{5}$$

where $B/A$ is the quadratic nonlinear parameter and $c_0(\mathbf{x})$ is the sound speed, that can be also spatially dependent.

In this system of equations, quadratic nonlinearity appears in the equation of motion (3) and in the continuity equation (4), in the momentum and mass advection terms respectively, and also in the equation of state, Eq. (5), relating pressure and density acoustic perturbations. We note that here we only take into account the nonlinear processes through the layer's bulk. The nonlinear effects at the boundary between adjacent sheets are neglected. These nonlinear boundary effects include cavitation processes, that in the case of fluids with very different compressibility can be very important. In the case of solid layers, other local nonlinear effects relative to boundaries, e.g., clapping phenomena between surfaces, can lead to local nonlinearities that are orders of magnitude higher in importance compared to the *bulk* cumulative nonlinearities.

### 2.2. The medium and its dispersion relation

We consider a periodic medium made of an arrangement of homogeneous and non-dissipative fluid layers of thickness $a_1$ and $a_2$ with different material properties both with the same density $\rho_0$. For the sake of simplicity, only longitudinal waves under normal incidence are considered. A scheme of the medium is shown in Fig. 1.

The propagation of small-amplitude waves in an infinite periodic system is completely described by its dispersion relation, often known as band structure, which for 1D systems as in Fig. 1 can be expressed analytically as [14]:

$$\cos(ka) = \cos(k_1 a_1)\cos(k_2 a_2) - \frac{1}{2}\left(\frac{k_1}{k_2} + \frac{k_2}{k_1}\right)\sin(k_1 a_1)\sin(k_2 a_2) \tag{6}$$

also known as the Rytov formula, where $k$ is the Bloch wave-number, $a = a_1 + a_2$ is the lattice period, and $k_i = \omega / c_i$ is the local wavenumber, with $c_i$ the sound speed in the $i$ layer. For a wave of frequency $\omega$ incident in a medium with known acoustic $c_i$ and geometrical $a_i$ parameters, the above equation results in a band structure of propagating and nonpropagating

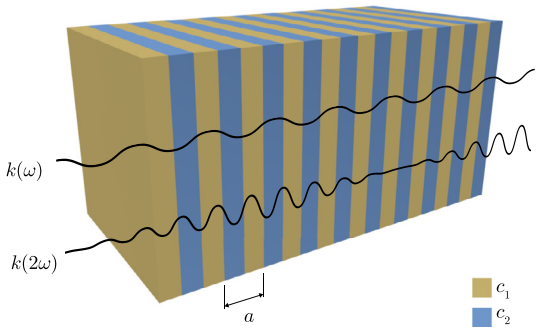


**Fig. 1.** Layered acoustic system with two different layers and second harmonic generation scheme. Here the lattice period is $a = \sum a_i$.

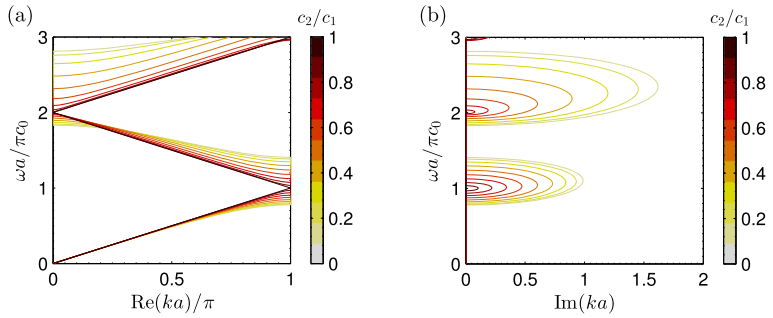


**Fig. 2.** Dispersion relation of the two-layers system for layer proportion $\alpha = 0.5$ and for different $c_2/c_1$ ratio. (a) real wavenumbers (band structure). (b) Imaginary part of the complex wavenumber (i.e. length of the exponential decay in the band-gap).

(band gap) regions, as shown in Fig. 2. Thus, using Eq. (6), we can estimate the effect of periodicity on the different harmonics of the incident wave as they propagate through the multilayer, which is the main premise of this work. The ratio between layer thickness can be defined as $\alpha = a_1/a$, leading to $a_2 = (1-\alpha)a$.

An example of dispersion relation plot is shown in Fig. 2 for the layer thickness ratio $\alpha = 0.5$ and for different sound speed ratios $c_1/c_2$. Increasing the impedance ratio between layers increases the reflected intensity at the multilayer, while the transmitted energy of the multiple internal reflections diminishes. As can be seen, due to these scattering processes, band gaps are progressively opened around the wavenumber $k = n\pi/a$, with $n = 1, 2, \ldots$. Thus, the bandwidth of these band gaps also increases when the impedance ratio grows.

On the other hand, its imaginary part increases in amplitude with $c_1/c_2$, leading to shorter evanescent propagation inside the band gap for high sound speed contrast layers, while it remains zero (no attenuation) in the propagation band. We recall that the system is conservative: the physical interpretation of the complex wavenumber is not energy absorption, but back reflection of the incident wave. Thus, at band gap frequencies, the waves penetrate only a short distance into the medium with a forward evanescent mode, and if the medium is perfectly periodic and lossless, the energy is back-reflected (it behaves as a mirror).

## 3. Harmonic generation in layered media

We will study the response of the layered system for plane-harmonic wave excitation. Then, as sketched in Fig. 1, the source is placed at one boundary of the layered system, and the acoustic-relevant magnitudes are calculated along space and time. As the wave propagates, cumulative nonlinear effects generate harmonics of the fundamental frequency, $\omega_0$, and due to the multiple scattering processes into the layers, local nonlinear effects also distort the wave. However, the high dispersion of the layered system has a strong impact on the nonlinear harmonic generation. Dispersion modifies the resonance conditions between fundamental and second-harmonic waves, and also for other nonlinearly generated higher frequencies. In this way, nonlinear energy transfer efficiency from one component to another is modified in a wide variety of configurations, leading to the possibility of engineering and controlling the nonlinear wave processes by tuning the dispersion relation.

Depending on the frequency of the incoming wave, different scenarios can be observed, as reported in the following subsections.

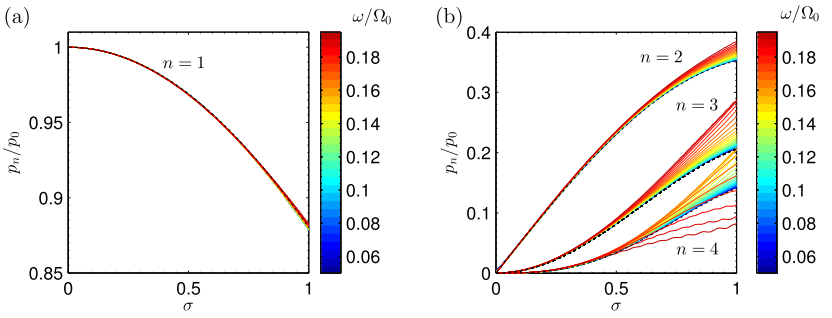


**Fig. 3.** Harmonic generation in the layered medium at low frequencies (numerical results in continuous colored lines), and its comparison with analytical expressions (Fubini) for an homogeneous medium (in dashed black line). The harmonic number is labeled as $n$.

### 3.1. Nondispersive (Fubini) regime

We start studying the propagation in the layered system for harmonic excitation in the very-low-frequency (long-wavelength) regime, where we assume that $ka \ll 1$ holds. As the Rytov's Eq. (6) predicts, in the very-low-frequency regime the slope of the $\omega(k)$ curve is nearly constant. In this limit, the dispersion of all the spectral components is negligible, they all propagate at nearly the same velocity and are correspondingly phase-matched. Thus, in the absence of dispersion and attenuation process, the system of Eqs. (1), (2), and (5) can be reduced for a harmonic-plane wave to the Burger's evolution equation expressed in traveling coordinates with effective parameters, namely $\tilde{c_0}$, $\tilde{\rho_0}$ and $\tilde{\beta}$. In the following, tildes will be removed to simplify the notation. An analytic solution of this equation in terms of the $n$th-harmonics of the fundamental wave of frequency $\omega$ and initial amplitude $p_0$ is known as the Fubini solution,

$$p(\sigma,\tau) = p_0 \sum_{n=1}^{\infty} B_n(\sigma)\sin(n\omega\tau) \tag{7}$$

where $B_n(\sigma) = (2/n\sigma)J_n(n\sigma)$ is the amplitude of the harmonic of order $n$, being $J_n$ is the Bessel function of order $n$, and $\sigma = x/x_s$ is the propagation coordinate, normalized to the shock formation distance, $x_s = \rho c_0^3/(\omega\beta p_0)$, that corresponds to the distance after which a plane wave develops a discontinuity (a shock) due to cumulative distortion, $\tau = t - x/c_0$ is a retarded time and $\beta = 1 + B/2A$ is a the parameter of nonlinearity that accounts for the nonlinearities in Eqs. (3)–(5). This celebrated solution is valid for $\sigma < 1$ (pre-shock region). More complex expressions, as the Blackstock solution, are valid in the whole domain [15], and will be used later.

All simulations presented in this work were carried out using the full-wave constitutive relations, Eqs. (1) and (2), together with the second-order expansion of the state equation, Eq. (5). We define the normalized reference frequency as $\Omega_0 = \pi c_0/a$ (located in the first band gap), where the effective sound speed in the low-frequency limit is given by the Taylor expansion of Eq. (6) around $k = 0$ as $c_0 = (ac_1^2c_2^2/(a_2c_1^2 + a_1c_2^2))^{\frac{1}{2}}$ [16].

Fig. 3 shows the analytical and numerical solutions for the low-frequency limit of the layered system, where an excellent agreement is obtained between Fubini and numerical solutions in the pre-shock region, $\sigma < 1$, and for low excitation frequencies, $\omega/\Omega_0 \ll 1$. However, when the fundamental frequency is increased, the higher harmonics fall into the dispersive region, and thus its wave speed is reduced. Consider the case of a source of frequency $\omega_0 = 0.2\,\Omega_0$, red curves in Fig. 3. In this situation, phase matching conditions are no longer fulfilled for all the spectral components and therefore the energy transfer from fundamental to higher harmonics is modified. In these conditions, dispersion affects the cumulative harmonic generation, leading to a decrease in the energy transfer from lower to higher harmonics. Dispersion, in general, is higher at higher frequencies, and thus the Fubini solution is no longer accurate to describe harmonic generation in this conditions. The Fubini solution can be only applied as an ideal solution for the low-frequency limit or as a good approximation for the first harmonics and for frequencies below $\omega \lesssim 0.1\,\Omega_0$, for which dispersion effects can be neglected for lower harmonics.

### 3.2. Dispersive regime

For frequencies above the validity of the (non-dispersive) homogeneous-Fubini regime, finite dispersion effects are observed. The dispersion of the layered system deeply affects the harmonic generation process.

As intense waves propagate through a quadratic nonlinear medium, their frequency components interact with each other and waves with new frequencies arise as a combination of the original frequencies, including higher harmonics. The cumulative energy transfer from the interacting waves to the harmonics is dependent on the resonance conditions $\omega_0 \pm \omega_1 = \omega_2$, $\mathbf{k}_0 \pm \mathbf{k}_1 = \mathbf{k}_2$. Note that these conditions express the laws of conservation of energy ($\hbar\omega$) and momentum ($\hbar\mathbf{k}$) in the quantum description for the disintegration and merging of quanta [13]. These conditions can be satisfied in a variety of situations. The most simple case is observed in nondispersive media and for collinear waves $k_i = \omega_i/c_0$. In this situation, the resonance conditions are fulfilled all over the spectra and a large number of harmonics interact synchronously: when

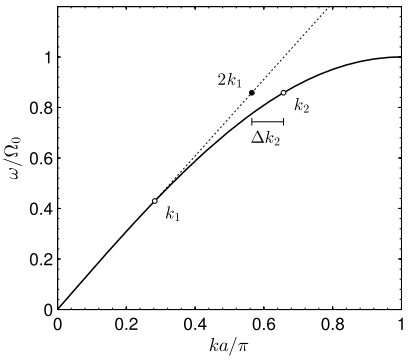


**Fig. 4.** Scheme of the phase miss-matching between the fundamental and the second harmonic waves. The fundamental wave vector $k_1$ at frequency $\omega$ generates a *forced* wave $2k_1$ at frequency $2\omega_0$. The *free* wave that the system allows to propagate is $k_2$, located in the dispersion relation curve. Due to dispersion, $k_2 \neq 2k_1$, and there is a phase mismatch, $\Delta k$ between both waves and the generation is therefore asynchronous.

there exist in the system a *free* wave with velocity $\omega_2/|\mathbf{k}_2|$ that matches the excited (*forced*) wave $\omega_0 \pm \omega_1/|\mathbf{k}_0 \pm \mathbf{k}_1|$, the *free* wave is excited in a resonant way. The resonant interaction leads therefore to synchronous (phase matched), cumulative energy transfer from the initial wave to the secondary wave fields.

In the case of an initial monochromatic wave, the main wave generates its second harmonic. The resonant condition in this situation reads, $2\mathbf{k}_1 = \mathbf{k}_2$, that holds true for nondispersive collinear waves, leading to a synchronous generation $\Delta k = k_2 - k_1 = 0$. However, in the case of dispersive media, this condition is, in general, not fulfilled and the *forced* and *free* waves interact asynchronously. Fig. 4 shows such situation for a layered media with a fundamental wave in the first dispersion band.

In order to study asynchronous second-harmonic generation processes analytically, a more convenient approach is to use an equivalent nonlinear wave equation, and finding its approximate solutions for the harmonics by a perturbation method. As shown, e.g., in [15], for moderate amplitudes, the system of Eqs. (3)–(5) can reduced to a single nonlinear wave equation,

$$\nabla^2 p - \frac{1}{c_i^2}\frac{\partial^2 p}{\partial t^2} - \frac{1}{\rho_0}\nabla\rho_0\nabla p = -\frac{\beta}{\rho_0 c_0^4}\frac{\partial^2 p^2}{\partial t^2} - \left(\nabla^2 + \frac{1}{c_0^2}\frac{\partial^2}{\partial t^2}\right)\mathcal{L} + \mathcal{O}(\varepsilon^3) \tag{8}$$

which is valid for nonhomogeneous media up to the second order. The parameter of nonlinearity is given by $\beta = 1 + B/2A$ and $\mathcal{L}$ is a Lagrangian energy density term defined as [15]

$$\mathcal{L} = \frac{1}{2}\rho_0 v^2 - \frac{p^2}{2\rho c_0^2} \tag{9}$$

The Lagrangian density vanishes for plane progressive waves, due to the first order relation $p = |v|c_0\rho_0$ holds and leads to $\mathcal{L} = 0$. In this case, Eq. (8) simplifies to the well-known (lossless) Westervelt equation for nonhomogeneous media

$$\nabla^2 p - \frac{1}{c_0^2}\frac{\partial^2 p}{\partial t^2} - \frac{1}{\rho_0}\nabla\rho_0\nabla p = -\frac{\beta}{\rho_0 c_0^4}\frac{\partial^2 p^2}{\partial t^2} + \mathcal{O}(\varepsilon^3) \tag{10}$$

In general, the Lagrangian density term can be discarded based on the distinction of cumulative and local nonlinear effects. In this way, for progressive quasi-plane wave propagation in homogeneous media, the nonlinear local effects become insignificant in comparison to the nonlinear cumulative effects, where in most practical situations, beyond a distance of only few wavelengths away from the source, local nonlinear effects can be neglected. In our case, the validity of Eq. (10) is confirmed when comparing its analytical predictions with the numerical solutions of the constitutive equations, as shown in Fig. 5, as shown below.

Analytical harmonic amplitudes can be obtained as solutions of the nonlinear wave equations, in particular the Westervelt equation, Eq. (10). For that aim, we expand the pressure field as a sum of contributions of different orders, i.e. $p = p^{(1)} + \varepsilon p^{(2)} + \cdots$, where $\varepsilon$ is the smallness perturbation parameter, which we identify with the acoustic Mach number, $\varepsilon = v/c_0$. Thus, $p^{(1)}$ is the first-order (linear) solution of the problem and $p^{(2)}$ its the second-order contribution. By substituting the expansion in the second-order wave, Eq. (10), assuming constant density[1] and neglecting $\mathcal{O}(\varepsilon^3)$ terms, we get a coupled set of equations that can be solved recursively. The solution of the first-order equation corresponds to a monochromatic plane wave of frequency $\omega$

$$p^{(1)} = p_0 \sin(\omega t - k_1 x) \tag{11}$$

[1] We neglect the ambient density variations for the sake of simplicity. Dispersion arise also for sound speed variations, that are assumed to be implicit in the boundary conditions.

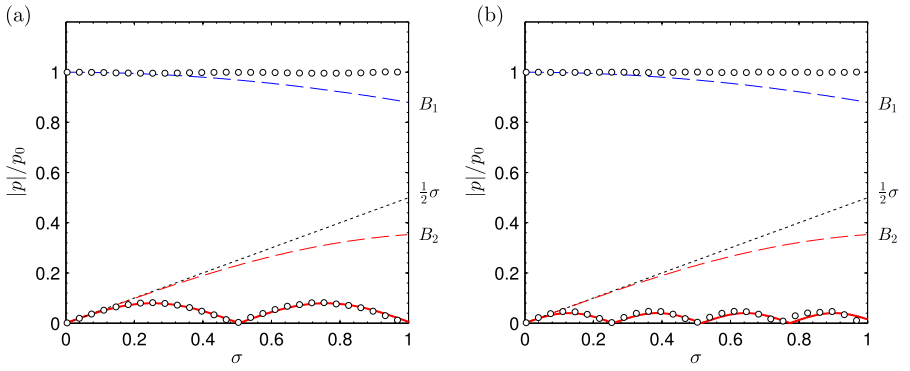


**Fig. 5.** Second harmonic evolution for (a) $x_c/x_s = 1/4$ and (b) $x_c/x_s = 1/8$ obtained using Eq. (15) (continuous red line), numerically (white circles), nondispersive linear law of growth (dotted line) and Fubini nondispersive solution, $B_2$ (dashed red). First-harmonic evolution has also been represented for the numerical (white circles), and (blue dashed) $B_1$ Fubini nondispersive solutions.

where $k_1 = k(\omega)$ is the wave vector associated with the primary frequency $\omega$, and $p_0$ is the excitation pressure amplitude. Substitution of the first-order solution into the equation obtained at the next order in the expansion, leads to an inhomogeneous equation for the second harmonic field:

$$\frac{\partial^2 p^{(2)}}{\partial x^2} - \frac{1}{c_0^2}\frac{\partial^2 p^{(2)}}{\partial t^2} = -\frac{4\beta\omega^2 p_0^2}{\rho_0 c_0^4}\sin(2\omega t - 2k_1 x) \tag{12}$$

The general solution of this equation is the sum of the solution of the homogeneous equation ($p_0 = 0$), and the particular solution of the inhomogeneous equation ($p_0 \neq 0$). Therefore, the field for the second harmonic can be expressed as $p^{(2)} = p_h^{(2)} + p_f^{(2)}$, where the corresponding waves for this two solutions are the *free*, and *forced* waves respectively. Such homogeneous and particular solutions are:

$$p_h^{(2)} = P_h^{(2)}\sin(2\omega t - k_2 x) \tag{13}$$

$$p_f^{(2)} = \frac{A}{(k_2 + 2k_1)(k_2 - 2k_1)}\sin(2\omega t - 2k_1 x) \tag{14}$$

where $k_2 = k(2\omega)$ is the wavenumber of the *free* wave at second harmonic frequency, and the constant $A = -4\beta\omega^2 p_0^2/\rho_0 c_0^4$. Note that as $2k_1 \neq k_2$, the *forced* and *free* waves in dispersive media have different phase speed, i.e. the *forced* and *free* waves are phase mismatched as can be seen in the argument of the sin function in Eqs. (13) and (14). Imposing the boundary condition, that the second harmonic must be absent at $x = 0$, the second harmonic field can be expressed as

$$p^{(2)} = \frac{A}{k_2 \Delta k}\sin\left(\frac{\Delta k}{2}x\right)\cos\left(2\omega t - k_2' x\right) \tag{15}$$

where the effective wave number is $k_2' = (k_2 + 2k_1)/2 \approx k_2$ and the detuning parameter that describes the asynchronous second harmonic generation is defined as

$$\Delta k = k_2 - 2k_1 = k(2\omega) - 2k(\omega) \tag{16}$$

Equation (15) describes the second-harmonic generation in dispersive media, that is the beating in space of the second harmonic field when the resonant conditions are not fulfilled. Thus, as $\Delta k$ increases, the spatial period of the beating and also its maximum amplitude decreases. The distance between the positions of the maxima of the beating, is called the coherence length, and can be related to the second-harmonic phase-mismatching frequency as:

$$x_c = \frac{\pi}{|\Delta k|} = \frac{\pi}{|k(2\omega) - 2k(\omega)|} \tag{17}$$

This length corresponds to the half of the spatial period of the beating, where the maximum of the field is located. It can be expressed also for the $n$-th harmonic simply as $x_c(n) = \pi/|\Delta k_n| = \pi/|k(n\omega) - nk(\omega)|$.

In the limiting case of $\Delta k \to 0$, the second-harmonic field is generated synchronously and accumulates with distance, so a linear growth is predicted. In this case, the phase matching condition is fulfilled and the *free* wave is excited synchronously to the *forced wave*. Note here that in the derivation of Eq. (15), only second-order processes are taken into account, and therefore only the amplitude of the second harmonic is predicted. This leads to overestimate the second harmonic field: as long as no energy is transferred to the third harmonic, the second harmonic predicted by Eq. (15) in the absence of dispersion grows indefinitely. The validity of this model can be explored, expanding the Bessel functions of Fubini series near

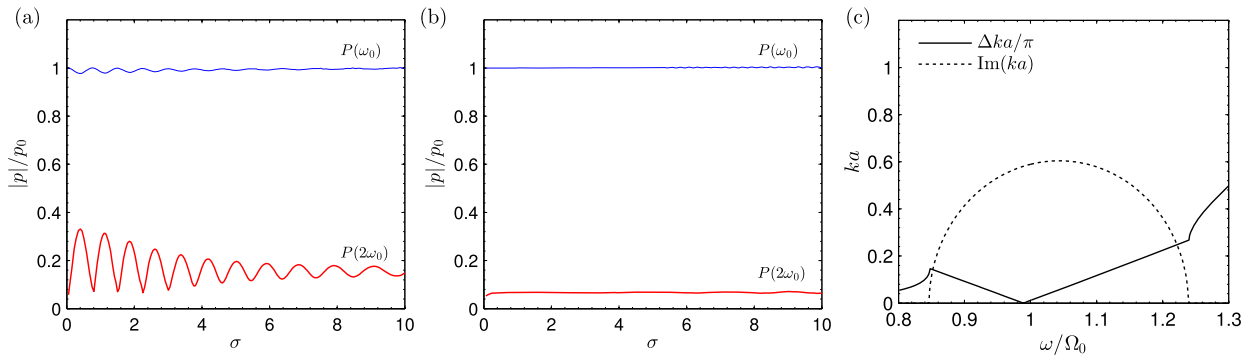


**Fig. 6.** Evolution of the second harmonic field propagating in band gap for second-harmonic frequencies (a) below the middle of the band gap $2\omega_0 = 0.84\,\Omega_0$, (b) in the middle of the band gap $2\omega_0 = \Omega_0$. All results for a layered medium with $\alpha = 1/2$ and $c_1/c_2 = 1/2$. (c) Detuning of the second harmonic (continuous line) and imaginary part (dotted line) in function of the normalized frequency.

the source. A simple comparison between the full Fubini solution and linear second-harmonic growth gives a reasonable approximation for distances $\sigma < 0.5$ or for second-harmonic field values satisfying $p(2\omega) < p_0/4$.

Fig. 5(a, b) shows two different simulations in the dispersive regime of the layered media where the wave amplitude and frequency has been selected to match $x_c/x_s = 1/4$ and $x_c/x_s = 1/8$, corresponding to $w_0 = 0.318\,\Omega_0$ and $w_0 = 0.363\,\Omega_0$. The layered media parameters were $\alpha = 0.5$ and $c_2 = c_1/2$. The waves with higher beating spatial period correspond to the lower frequencies. The analytical solution for the second harmonic matches the full-wave numerical solution. However, differences can be observed in the second harmonic amplitude estimation for $x_c/x_s = 1$ (left plot in Fig. 5). This overestimation by the analytical solution can be related to the absence of energy transfer to higher harmonics, which is not considered by the perturbation solution but is included in the simulation. Therefore, this model is specially suitable in situations where the third harmonic does not grow cumulative with distance. In the lossless layered media, this situations include frequencies that lead to very high third-harmonic mismatch and also when the third harmonic falls in the band gap.

### 3.3. Second harmonic in band gap

Waves with frequencies falling into the band gap of the dispersion relation are evanescent due the non-negligible imaginary part of its complex wave number. Thus, its amplitude decays exponentially with distance. If the nonlinearly generated second harmonic falls into a band gap, its amplitude does not decay, but reaches a constant value [5]. Fig. 6 shows this case for two different frequencies. The constant amplitude value of the second harmonic wave depends on the imaginary part of the wave vector.

This effect can be understood in terms of the *free* and *forced* waves. If the second harmonic is evanescent (as follows from the dispersion relation), the wave will not accumulate with distance. The fundamental wave is "pumping" energy to the second harmonic field at every point in space. Thus, the second harmonic field is generated locally and remains trapped inside the layered media. It reaches a constant level that depends on three main factors. In first place, the "pumping" rate, characterized by the fundamental wave amplitude and medium nonlinearity, or more strictly the ratio between the layer thickness and the shock distance $a/x_s$. Secondly, it also strongly depends on the magnitude of the imaginary part of the complex wave number, i.e. the ratio between its characteristic exponential decay length and the shock distance in a layer. The characteristic decay length of the evanescent propagation is always shorter when the second harmonic is in the middle of the band gap, leading to a weaker second-harmonic field in this frequency region, as seen in Fig. 6. Finally, it depends also on the detuning of the real part of the wave number, where for the first band the gap is minimum at the center. The first factor can be isolated and studied separately. However, the two last factors are linked through the specific dispersion relation of the medium.

Fig. 6c shows the detuning of the second harmonic and the imaginary part as a function of the frequency for a medium with $\alpha = 1/2$ and $c_1/c_2 = 1/2$, showing that at the middle of the band gap these two factors have opposite effects: detuning is null (phase matching) when evanescent decay is nearly maximum, and vice versa. However, the magnitude of the effects can be very different. As the rate of the second harmonic generation (see the initial slope in Fig. 5) is independent of the detuning, and the evanescence implies that the wave decays after few layers, there is no practical compensation for the effects at the center of the band gap. However, the situation is different for frequencies around the limits of the band gap, where the coherence length is of the order of the exponential decay characteristic length. Thus, for frequencies below the middle of the bad-gap and for amplitudes with shock distance comparable to the evanescent characteristic decay length, the beatings can be also observed, as shown in Fig. 6a. Then, if frequency is increased, the characteristic decay length becomes shorter than the shock wave distance and beatings cannot be observed, leading to the characteristic constant second harmonic field shown in Fig. 6b.

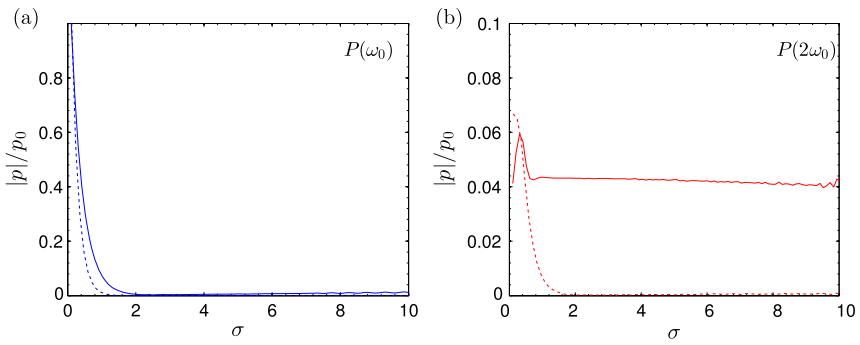


**Fig. 7.** (a) Evolution of the fundamental harmonic wave field with its fundamental frequency falling below the middle of the band gap and in the band gap, $\omega_0 = 0.87\,\Omega_0$, (continuous line), and in the middle of the bad-gap, $\omega_0 = \Omega_0$ (dotted line). (b) Corresponding second harmonic field, where for $\omega_0 = \Omega_0$ (dotted line) second harmonic frequency falls in the 2nd band gap while for $\omega_0 = 0.87\,\Omega_0$, (continuous line) lies into a propagating band.

### *3.4. Fundamental harmonic in band gap*

When the fundamental frequency of the wave lies within the band gap, small-amplitude waves propagate evanescently. Essentially, the same applies to finite-amplitude harmonic waves. In general, if the shock distance is large compared to the characteristic decay length of the evanescent wave, the nonlinear effects have no chance to accumulate and harmonic amplitude is negligible. Since the characteristic exponential decay is about a few lattice sites, this means that the initial amplitude necessary to achieve nonlinear effects in this configuration is much higher than those in the preceding sections. Fig. 7 shows the evolution of the first- and second-harmonic waves for a fundamental frequency at the Bragg frequency, $\omega_0 = \Omega_0$ at a frequency just below the middle of the band gap and in the band gap, $\omega_0 = 0.87\,\Omega_0$ for a layered media of $\alpha = 1/2$ and $c_1/c_2 = 1/2$. In the first case, the imaginary part of the wave vector is remarkable high and the waves decay fast after a few lattice units. Due to this fast decay, the second harmonic interacts only over a short distance with the first, and its amplitude is very limited. After a few lattice units, the fundamental wave can be treated as a small-amplitude evanescent wave. The second harmonic, which also falls in the band gap (but in the second band gap), also decays exponentially.

On the other hand, if the fundamental frequency is set just below the middle of the band gap, where the imaginary part of the wave-vector is smaller that in the center, the amplitude of the fundamental wave decays more slowly, penetrating deeper into the material. The interaction region with the second harmonic is larger, and nonlinear effects result in a more efficient generation of the second harmonic. In this configuration at $\omega_0 = 0.87\,\Omega_0$, the second harmonic does not fall inside a band gap. Therefore, the generated second-harmonic wave at the beginning of the lattice propagates through the medium essentially without amplitude change. Due to the evanescence of the fundamental wave, there is only *forced* wave at the beginning of the medium. Therefore, although in this configuration waves are phase mismatched, beatings are not present: only the *free* wave propagates through the medium.

## 4. Nonlinear acoustic field management

### *4.1. Tuning nonlinearity with dispersion*

In the preceding sections, we have explored the fundamental behavior of nonlinear waves generated inside the layered media. But also, medium parameters can be designed to provide specific conditions. The material parameters can be tuned to get coherence at one frequency of interest, e.g., at one of the harmonics of the fundamental wave, or to get detuning or evanescent propagation at other specific harmonics. Using these mechanisms, the layered medium can be used to provide a balance of the harmonic amplitudes, or to obtain specific nonlinear waveforms, providing a control of the nonlinear process inside the medium.

In the design of a system for this purpose, the coherence length is a useful control parameter. To this aim, the analytic Eq. (6) is used, which is shown to provide an excellent framework to tune the layered parameters to obtain the desired balance between detuning, evanescent propagation, synchronous generation and, at the same time, it allows us to find those conditions for a specific phase/group speed. Fig. 9a shows an example of the dispersion relation of a multilayer system, and Fig. 9b the corresponding coherence length for the second and third harmonics. The resulting harmonic amplitudes when phase matching of all harmonics is achieved is shown in Fig. 8. This happens for a set of frequencies $\omega = (0, 1.75, 2.333, \ldots)\,\Omega_0$, marked by triangle in Fig. 9b. At this frequency, coherence is recovered and the phase matching conditions are fulfilled. Therefore, the nonlinear generation of higher harmonics in the multilayer media in these conditions is equivalent to that in a homogeneous (nondispersive) medium, as shown in Fig. 8.

On the other hand, for some frequencies there is coherence for the second, but a non-negligible detuning is observed for the third. The opposite effect can also be obtained, where coherence is achieved for the third harmonic, but the second harmonic presents strong dispersion. Finally, other interesting regions are those where the second harmonic component is almost phase matched and, for the same frequency the third harmonic falls into a band gap.

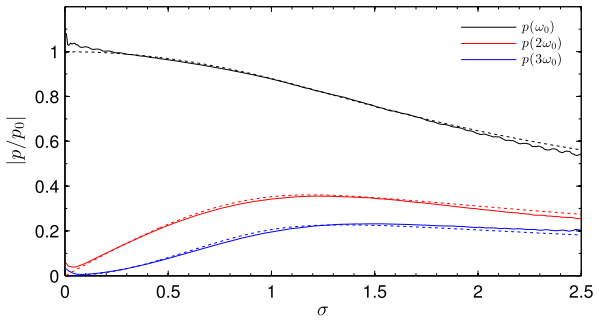


**Fig. 8.** Harmonic distribution for the frequency $\omega_0 = 1.75\,\Omega_0$. Coherence is recovered for at least the lowest spectral components. Blackstock solution (dotted lines).

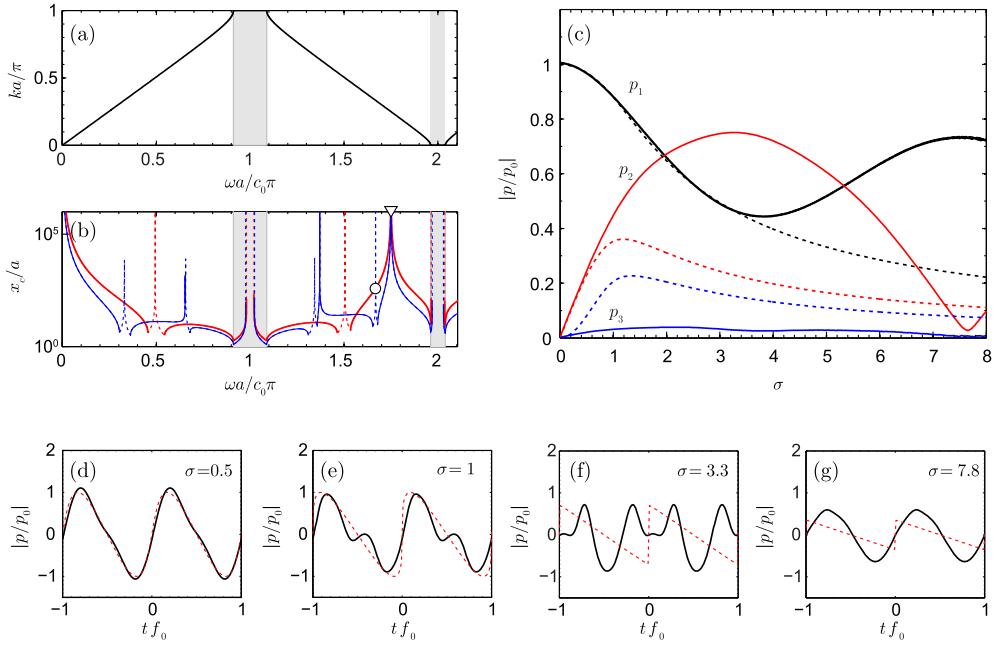


**Fig. 9.** (a) Dispersion relation for a layered media of $c_1/c_2 = 1.33$ and $\alpha = 1/2$. (b) Coherence length for second (red) and third (blue) harmonics as a function of the fundamental frequency normalized to the lattice period $a$. Phase matched frequencies are those with $x_c/a \to \infty$, and asynchronous generation is predicted for $x_c \to 0$. Frequencies at which the fundamental frequency is in band gap are marked in gray regions, while band gap regions for second and third harmonic are marked by dashed lines. (c) Harmonic distribution for $\omega_0 = 1.668\,\Omega_0$ where a coherence is achieved for the second harmonic and the frequency of the third harmonic falls into the band gap. (d–g) (continuous lines) Waveforms at different distances. At $\sigma = 3.3$, the second-harmonic generation field is maximized and the frequency doubling in the waveform can be seen in (f). Then, as shown in sub-panel (g), at $\sigma = 7.8$, due to second-harmonic detuning, a nearly sinusoidal wave is recovered. Analytic Fubini–Blackstock solutions for the harmonics (red dotted lines) are plotted for comparison. Time coordinate in (d)–(g) $\tau = tf_0 = t/T_0$ is normalized to the period of the fundamental wave.

In the following subsections, we propose and analyze different configurations of the layered medium with specific balance between detuning, evanescent propagation, and synchronous generation.

### *4.2. Enhanced second harmonic generation*

One can expect that the second harmonic generation is maximized in homogeneous nondispersive media. However, in nondispersive media coherence is achieved not only at second-harmonic frequency, but also in the higher spectral components. As a result, energy is transferred from second harmonic field to higher spectral components, and therefore the second-harmonic field does not grow indefinitely. Moreover, shock waves are formed and nonlinear absorption reduces wave intensity for $\sigma > \pi/2$ even in lossless media [15].

The dispersion of the layered system can be used to modify this situation by including phase mismatches that alter the higher harmonic cascade processes, while maintaining coherence for the second harmonic. Fig. 9a–b shows an example of a dispersion relation where for $\omega_0 = 1.668\,\Omega_0$ (marked by a white circle in Fig. 9b) it can be observed that there is a high coherence for the second harmonic ($x_c/a \approx 1000$), while the third harmonic falls in a band gap. Fig. 9c shows the harmonic distribution in this situation. Here, energy is transferred to the second-harmonic field that grows almost linearly for $\sigma < 2$.

On the other hand, the energy transferred from the second to the third harmonic is not cumulative and its amplitude does not grow with distance. The third harmonic has evanescent propagation due to the imaginary part of the complex wave vector at this frequency. A constant field, as studied in Sec. 3.3, is obtained for the third harmonic.

The maximum amount of the second-harmonic amplitude in nondispersive media is $p_2|_{\max} \approx 0.36 p_0$, while in the example of Fig. 9c a maximum second-harmonic amplitude of $p_2|_{\max} \approx 0.75 p_0$ is predicted. As it is shown in Fig. 9c, the decrease in the first harmonic follows the analytic nondispersive Blackstock solution for $\sigma \lessapprox 3$. Thus, in this regime all the energy of the first harmonic is being transferred to the second-harmonic field. However, due to finite detuning of the second harmonic, a long spatial beating is produced, with normalized period $7.8\sigma$, and the energy is returned back to the first harmonic component.

We recall that at a distance $\sigma \approx 3$ a sawtooth profile is observed in the nondispersive media. In contrast, only second and first harmonics have remarkable amplitude into the layered media. The energy transfer to higher harmonics is therefore modified. Waveforms are shown in Fig. 9d–g. Near the source, where the amplitude of higher harmonics in not relevant, the nondispersive waveform (in red dotted) is well approximated by the fundamental and its second harmonic of the layered medium. However, due to the evanescent propagation of the third harmonic for longer distances, the nonlinear solution of the layered medium is mainly composed by the fundamental and its second harmonic. The amplitude of the maximum second harmonic in this configuration is observed at $\sigma = 3.3$, as it can be appreciated in the waveforms of Fig. 9 the frequency doubling. Moreover, due to finite detuning of the second harmonic, the process is not cumulative for all distances and at $\sigma = 7.8$ the energy is restored in the first harmonic again and a sinusoidal wave is obtained. Note that not all the energy is restored to the first harmonic in Fig. 9 at $\sigma = 7.8$, leading to a sinusoidal wave of different amplitude, as can be observed in Fig. 9a. The energy loss is mainly due to the artificial (numerical) viscosity necessary to nonlinear convergence [16]. For these simulations, the total distance is 1200 lattice sites and therefore the effects of attenuation are not negligible. However, the main nonlinear effects related to strong lattice dispersion are still appreciated. An analogous effect has been also studied in [13], where instead of dispersion, selective absorption at specific frequencies is used to modify and enhance harmonic generation.

### 4.3. Enhanced third-harmonic generation

In the first band ($\omega < \Omega_0$), coherence is always lower for the third harmonic than for the second. However, in the superior bands, the layered medium parameters can be tuned to obtain higher coherence for the third than for the second harmonic. Essentially we follow the same ideas as in the preceding section but for the third harmonic. In this case, the lattice is designed forcing the second harmonic to fall in the band gap. At the same time, perfect coherence can be found for the third harmonic at $\omega = 1.4\,\Omega_0$. This situation is illustrated in Fig. 10 around $\omega = 1.4\,\Omega_0$. In this case, the dispersion relation was obtained for a layered medium with parameters $\alpha = 0.3$ and $c_2/c_1 = 1/3$.

In this situation, as Fig. 10 shows, the second-harmonic wave attains a constant value of about $0.04 p_0$. As discussed in Section 3.3, this constant field does not grow with distance and is related to the evanescent solution of the *free* wave and the local nonlinear "pumping". On the other hand, due to the coherence of the third harmonic, all the energy transferred from the second to the third is accumulated with distance. Therefore, near the source, the rate of energy transfer from the second to the third harmonic is constant. Thus, the third harmonic starts to grow almost linearly with distance, opposite to quadratically as it does in homogeneous media.

Numerical simulations also show the fourth and fifth harmonic growth (not shown in Fig. 10), but only the fifth harmonic reaches a remarkable amplitude, growing near the source almost quadratically with distance. Therefore, the entire system behaves as an artificially cubic-like nonlinear medium formed by quadratic nonlinear layers.

The corresponding waveforms measured at $\sigma = (0.5, 2, 8, 12)$ are shown in Fig. 10d–g. For $\sigma = 0.5$ and 2, it can be observed how the wave steepens with the characteristic shape of cubic nonlinearity. No shock waves are formed as long as strong dispersion is present for high-frequency harmonics. It is worth noting here a remarkable fact: it steepens in the positive time axis direction (to the right in the figure), opposite than the quadratic nonlinearity plotted in red dotted as a reference. This effect, i.e. the steepening on the opposite side of the propagation direction, is characteristic of materials with negative parameter of nonlinearity. Therefore, the effective nonlinear behavior observed by the simulations in this conditions can be described as negative-cubic-like nonlinearity.

## 5. Conclusions

The interplay of dispersion and nonlinearity in multilayered periodic media, such as one-dimensional phononic crystals or superlattices, is shown to have a strong impact on the acoustic waves propagating through the structure. Nonlinearly generated harmonics propagating at different velocities are phase-mismatched, modifying the transfer of energy between the different harmonics, and therefore the waveform itself. Shock formation, typical of nonlinear homogeneous media, is in this way avoided. We propose a model and some particular solutions to study this problem, and report examples of configurations that result in an effective control of the spectrum of nonlinear acoustic waves by tuning the dispersion relation of the medium. Selective enhancement of second or third harmonic is demonstrated, leading in some cases to situations where the structure behaves with an effective nonlinearity different from that of its constitutive elements.

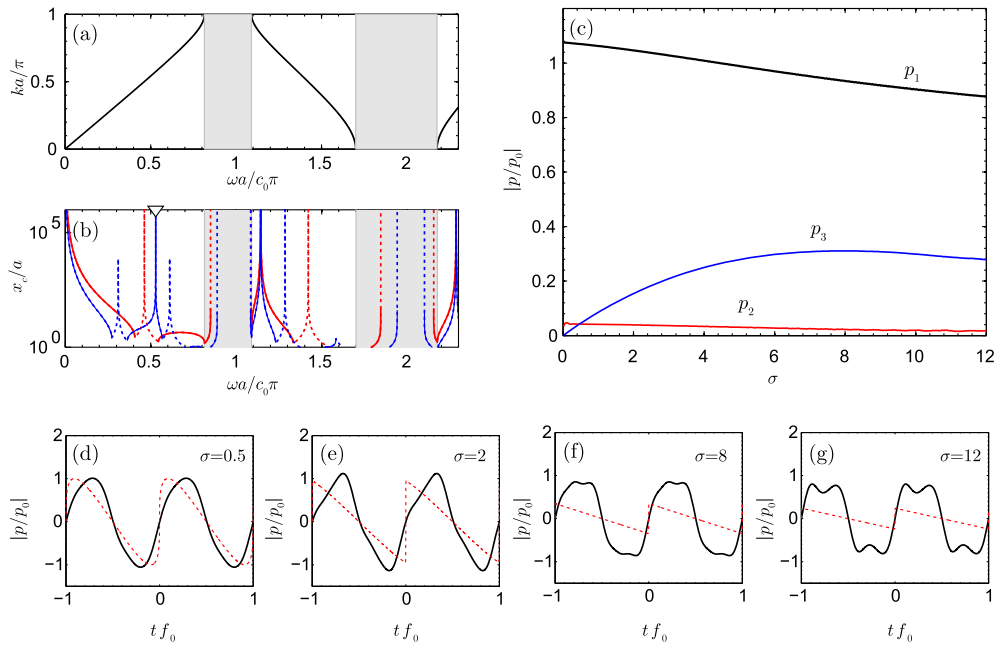


**Fig. 10.** (a) Dispersion relation for a layered media of $c_1/c_2 = 1/3$ and $\alpha = 0.3$. (b) Normalized coherence lengths for second (red) and third (blue) harmonics, (c) Harmonic distribution for $\omega_0 = 0.529/\Omega_0$ where a coherence is achieved for second harmonic, while the frequency of the third harmonic falls into the band gap. Bottom: (continuous lines) Waveforms at different distances for $\omega_0 = 0.529/\Omega$. At $\sigma = 3.3$, the second-harmonic generation field is maximized and a doubling of the waveform can be seen in the waveform. Then, at $\sigma = 7.8$, due to second-harmonic detuning, a nearly sinusoidal wave is recovered. Analytic Fubini–Blackstock solutions for the harmonics (red dotted lines) are plotted for comparison.

Work supported by Spanish Ministry of Economy and Innovation and European Union FEDER through projects FIS2011-29731-C02-02 and MTM2012-36740-C02-02. AM and LMGR acknowledge Generalitat Valenciana under grants Santiago Grisolia program (grant 2012/029) and BEST2015/279 respectively. RP and VJSM acknowledge the Spanish Ministry of Economy and Innovation under grants CAS14/00232 and PRX14/00705 respectively.

## References

[1] C. Kittel, Introduction to Solid State Physics, Wiley Eastern Limited, 1987.
[2] E. Yablonovitch, Inhibited spontaneous emission in solid-state physics and electronics, Phys. Rev. Lett. 58 (1987) 2059.
[3] M.M. Sigalas, E.N. Economou, Elastic and acoustic wave band structure, J. Sound Vib. 158 (1992) 377–382.
[4] V.J. Sánchez-Morcillo, I. Pérez-Arjona, V. Romero-García, V. Tournat, V.E. Gusev, Second-harmonic generation for dispersive elastic waves in a discrete granular chain, Phys. Rev. E 88 (2015) 043203.
[5] Y. Yun, G.Q. Miao, P. Zhang, K. Huang, R.J. Wei, Nonlinear acoustic wave propagating in one-dimensional layered system, Phys. Lett. A 343 (2005) 351–358.
[6] R.J. Leveque, D.H. Yong, Solitary waves in layered nonlinear media, SIAM J. Appl. Math. 63 (2003) 1539–1560.
[7] B. Liang, B. Yuan, J.-ch. Cheng, Acoustic diode: rectification of acoustic energy flux in one-dimensional systems, Phys. Rev. Lett. 103 (2009) 104301.
[8] E.M. Hamham, N. Jiménez, R. Picó, J. Sánchez-Morcillo, L.L.M. García-Raffi, K. Staliunas, Nonlinear self-collimated sound beams in sonic crystals, Phys. Rev. B 92 (2015) 054302.
[9] A. Huynh, B. Perrin, A. Lemaître, Semiconductor superlattices: a tool for terahertz acoustics, Ultrasonics 56 (2015) 66–79.
[10] A. Fainstein, N.D. Lanzillotti-Kimura, B. Jusserand, B. Perrin, Strong optical mechanical coupling in a vertical GaAs/AlAs microcavity for subterahertz phonons and near-infrared light, Phys. Rev. Lett. 110 (2013) 037403.
[11] A. Huynh, N.D. Lanzillotti-Kimura, B. Jusserand, B. Perrin, A. Fainstein, M.F. Pascual-Winter, E. Peronne, A. Lemaître, Phys. Rev. Lett. 97 (2006) 115502.
[12] W. Maryam, A.V. Akimov, R.P. Campion, A.J. Kent, Dynamics of a vertical cavity quantum cascade phonon laser structure, Nat. Commun. 4 (2013) 2184.
[13] K. Naugolnykh, L. Ostrovsky, Nonlinear Wave Processes in Acoustics, Cambridge University Press, 1998.
[14] A.M. Kosevich, The Crystal Lattice: Phonons, Solitons, Dislocations, Superlattices, John Wiley and Sons, 2006.
[15] M.F. Hamilton, D.T. Blackstock, Nonlinear Acoustics, Academic Press, San Diego, 1998.
[16] N. Jiménez, Nonlinear acoustic waves in complex media, Ph.D. Thesis, Universidad Politécnica de Valencia, Spain, 2015.